Scanning tunneling spectra of impurities in the Fe(001) surface

N. Papanikolaou,[1] B. Nonas,[1] S. Heinze,[1,2] R. Zeller,[1] and P. H. Dederichs[1]
[1]*Institut für Festkörperforschung, Forschungszentrum Jülich, D-52425 Jülich, Germany*
[2]*Zentrum für Mikrostrukturforschung, Universität Hamburg, D-20355 Hamburg, Germany*
(Received 16 December 1999; revised manuscript received 25 May 2000)

We present *ab initio* calculations of scanning tunneling spectra for the Fe(001) surface and for 3*d* impurities in this surface. The calculations are performed by the full-potential Korringa-Kohn-Rostoker Green's-function method, and also partly by the full-potential linearized augmented-plane-wave method. For the clean Fe(001) surface we demonstrate that the correct tunneling spectrum is only obtained in a full potential treatment, while the atomic-sphere approximation yields incorrect results. For 3*d* impurities in the surface layer, peaks appear in the spectra due to surfacelike states localized on the impurity site. Our results can explain recent scanning tunneling microscopy experiments on Cr impurities in the Fe(001) surface, and predict that chemical identification is also possible for many other transition-metal impurities.

I. INTRODUCTION

Since its first realization in the beginning of the 1980s scanning tunneling microscopy (STM) has become one of the most powerful tools in the study of surface phenomena. While semiconductor surfaces received the most attention, metallic systems were also studied extensively, and many problems in epitaxial growth of crystals as well as catalytic processes were resolved with the atomic resolution of the STM.[1]

The tunneling current depends on the electronic density of states near the Fermi level, as first pointed out by Tersoff and Hamann.[2] This makes chemical identification rather difficult,[3,4] and sometimes it is even impossible to deduce the atomic positions from a STM image.[5] In metals, tunneling via discrete states for high-bias voltages was used to obtain elemental contrast;[6] however, the required high voltages tend to reduce the resolution, so that it is difficult to identify single atoms with this method.

In some simple systems, element specific surface states close to the Fermi level can be directly observed in the tunneling spectra. For instance, this is the case in the bcc(001) surfaces of Fe and Cr.[7] Theoretical study gave a more detailed understanding of the observed resonances. In the case of Fe these surface states, which are of $s-d_{z^2}$ character, are energetically located in the band gap of the Δ_1 bulk minority states at the Γ point of the Fe band structure.[7] Similar surfacelike states were used to identify directly single Cr atoms on the Fe(001) surface with STM,[8] while analogous resonances were observed on a Fe(001) surface alloyed with Si.[9]

The ground-state properties of single impurities on the Fe(001) surface were recently studied theoretically.[10] For 3*d* and 4*d* impurities it was found that impurities from the beginning of the series couple antiferromagnetically to the Fe moments, while impurities from the end of the series couple ferromagnetically. Total-energy calculations showed that for most 3*d* impurities the adatom position is instable against a direct exchange mechanism, resulting in an integration of the impurities into the first layer, as observed experimentally for Cr impurities.[8]

A reliable analysis of the tunneling current can be done with the help of *ab initio* calculations.[7,9,4,11] STM essentially probes the surface electronic structure in the tip region. Despite the fact that a realistic description of the STM current taking into account the electronic structure of both sample and tip is rather difficult, reliable albeit more qualitative results can be obtained by the Tersoff-Hamann method. In this approach, which is based on a free-electron-like tip, the tunneling spectrum is directly connected with the local density of states in the tip position.[2]

The present paper has a twofold aim. First we recalculate the scanning tunneling spectra (STS) of the clean Fe(001) surface, and demonstrate that in agreement with previous theoretical results[7] the peak position of the surface state in the vacuum region is in good agreement with experimental STS findings. However, this agreement is only obtained if a full-potential procedure [like the full-potential Korringa-Kohn-Rostiker (KKR) or the full potential linearized augment plane-wave (FLAPW) method] is used. The standard atomic-sphere approximation for the potential yields the surface peak at an energy below the Fermi level. This could probably explain why the recent calculation of Fang *et al.*[12] failed to obtain agreement with the experimental data. Second, we calculate the electronic structure of 3*d* impurities in the Fe(001) surface. Here our aim is to explain the recent STS results for Cr impurities in the first Fe layer, which allow a chemical identification of the impurities. The calculations yield the experimental position of the impurity ''surface'' peak, and the origin of this impurity state is discussed. Our results show that similar peaks also occur for many other transition metal impurities in the Fe(001) surface, thus allowing a chemical identification of many more systems.

II. CALCULATIONAL METHOD

The tunneling current depends on the overlap between sample and tip wave functions. Assuming a spherical potential well for the tip, Tersoff and Hamann showed that the tunneling current $I(\mathbf{r}_\parallel, z; V)$ in a position $\mathbf{r}_\parallel$ at a distance z above the surface and at bias voltage V is

$$I(\mathbf{r}_\parallel,z;V)\propto\int_{E_F}^{E_F+eV} n(\mathbf{r}_\parallel,z;\epsilon)d\epsilon, \quad (1)$$

where E_F is the Fermi energy. From the above equation it is obvious that the local density of states $n(\mathbf{r}_\parallel,z;\epsilon)$ in the tip region is directly connected to the measured spectrum

$$dI/dV\propto n(\mathbf{r}_\parallel,z;E_F+eV). \quad (2)$$

The full-potential KKR Green's-function method is used to calculate the electronic structure of impurities on surfaces.[13,14] Exchange and correlation effects are treated within the local density approximation with the parameterization of Vosko *et al.*[15] Space is divided into ideal lattice atomic polyhedra, the correct shapes of which are taken into account by the use of shape functions.[16] A site-centered representation and a multipole expansion is used for the Green's function with an angular momentum cutoff $l_{max}=3$. This imposes a cutoff of $2l_{max}=6$ for the potential and the charge density, which naturally restricts the expansion up to $4l_{max}=12$ for the shape function. This angular momentum cutoff is sufficient to obtain well-converged results for the density of states in the vacuum region. First we calculate the electronic structure of ideal bcc bulk Fe in the theoretical lattice constant of 5.22 a.u. We then create two identical (001) surfaces by removing 9 ML of Fe, thus leaving two well-separated half crystals. The electronic states in the vacuum region as well as in the three first surface layers on each side embedded in ideal bulk Fe were calculated solving a Dyson equation for each $\mathbf{q}_\parallel$ point in the irreducible surface Brillouin zone.[13]

Introducing an impurity atom in the surface breaks the two-dimensional periodicity. Such a nonperiodic impurity problem can be elegantly treated with the Green's-function method. A description of the method and applications in other systems, using a spherical potential, can be found in Refs. 10, 14, 17, and 18. A cluster containing the impurity, and the first and second Fe neighbors around, as well as the vacuum region up to 5.5 Å above the impurity atom, was calculated self-consistently with the above full-potential Green's-function scheme. This includes 28 sites in total, with the impurity, 13 Fe atoms, and 14 empty atomic polyhedra in the vacuum region. This cluster of perturbed potentials is embedded in the unperturbed Fe(001) surface, which is described by the surface Green's function. Lattice relaxation effects of the surface layers as well as in the vicinity of the impurity are ignored in the present work, and the Fe atoms are located at the ideal bcc positions.

In order to test the accuracy of the KKR method, we also performed calculations with the FLAPW method[19] for the Fe(001) surface. The same method was used very successfully in the past[20] to predict the STM images of Fe surfaces. In this calculation the surface was modeled by a 31-layer film which is sufficient to have a good approximation of the surface, and more important minimize the influence of spurious size quantization effects which are present in finite-size slab calculations.

III. Fe(001) SURFACE

First we discuss our results for the pure Fe(001) surface. Previous *ab initio* calculations using the FLAPW method obtained good agreement with the experimental data.[7,9] Conversely, our first attempt to reproduce the measured tunneling spectra using the atomic-sphere approximation (ASA) failed to give the correct energetic position of the Fe(001) minority surface state close to E_F. It is often supposed that the ASA, despite its deficiency to describe a highly nonsymmetric environment, could still give accurate densities of states and charge densities even for surfaces. However the limits of validity of this approximation is not checked very often.

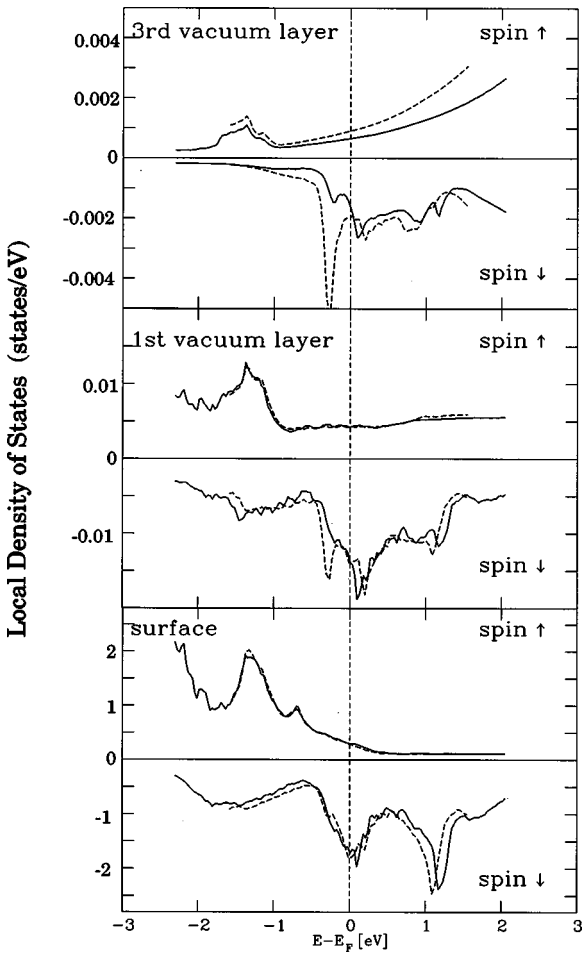

FIG. 1. Local density of states of an Fe(001) surface calculated with the KKR method using the atomic-sphere approximation (ASA, broken line) and the full-potential (FP, full line). From bottom to top, Fe(001) surface layer, first vacuum layer, and third vacuum layer.

In Fig. 1 we present the local density of states (LDOS) within an atomic volume for the surface layer, the first vacuum layer, and the third vacuum layer of Fe(001) calculated with the KKR-ASA and full potential (KKR-FP) using an angular momentum cutoff $l_{max}=3$.[21] In the KKR-ASA the potential is considered to be spherical within atomic spheres, but in the construction of the ASA potential we include the ''full'' charge density in the atomic sphere by using a multipole expansion up to $l=6$. The KKR-FP calculation was performed by taking into account both the full anisotropy of the potentials and the correct shape of the atomic polyhedra as described above. The differences between the two calculations shown in Fig. 1 for the surface layer are rather small, and only a small shift of the minority

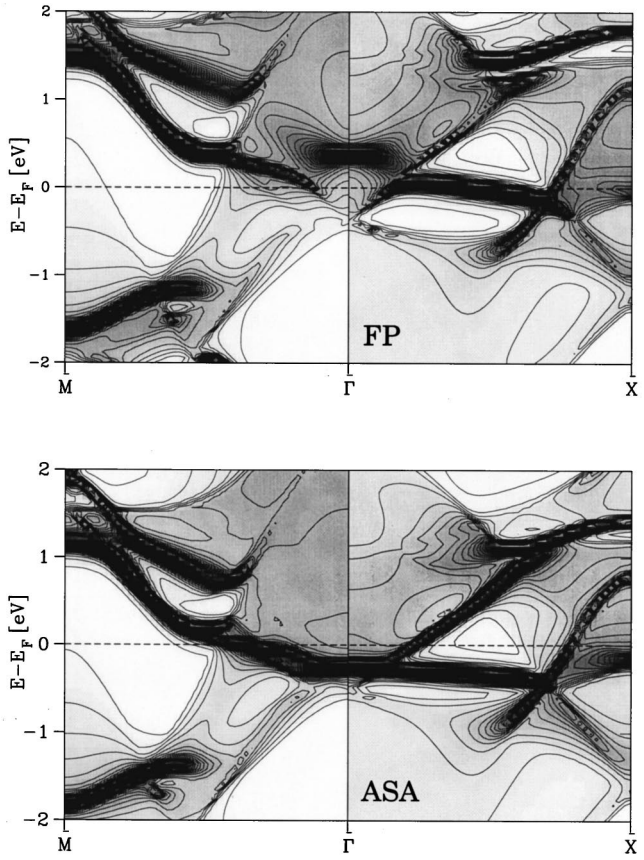

FIG. 2. Contour plot of the minority density of states $n(\mathbf{q}_\parallel, E)$ with even symmetry (with respect to a mirror plane along the high-symmetry line), along $\bar{\Gamma}$-$\bar{X}$ and $\bar{\Gamma}$-$\bar{M}$ of the 2D Brillouin zone of bcc(001), calculated with the KKR method. Dark regions correspond to high density. Comparison between full-potential (FP) and ASA calculations.

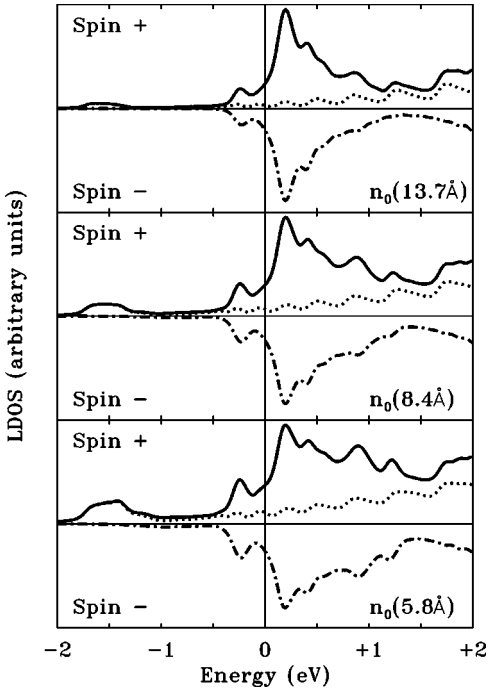

FIG. 3. Local density of states of Fe(001), calculated with the FLAPW method, at three different distances from the surface. Dotted line: majority DOS; dashed-dotted line: minority DOS; full line: total DOS. A finite slab of 31 ML of Fe with the same lattice constant of 5.22 a.u. as in the KKR calculation has been used.

unoccupied states is observed. However, in the vacuum region especially in the minority band, the difference becomes significant. The error can be clearly seen in the third vacuum layer where the ASA calculation results in a strong peak, just below the Fermi level in contradiction with the experimental results and the FLAPW calculations.[7,9] The KKR full-potential treatment is substantially better, predicting a peak just above the Fermi level, in agreement with the experimental observation. A peak just below E_F is also seen, but with a much reduced intensity.

In order to further investigate the origin of this failure of ASA to describe states that extend in the vacuum region, we have compared the projected density of states for the Fe surface layer, and for $\mathbf{q}_\parallel$ vectors along the $\bar{\Gamma}$-$\bar{M}$ and $\bar{\Gamma}$-$\bar{X}$ high-symmetry directions in the bcc(001) surface Brillouin zone. The KKR results are shown as contour plots for modes of even symmetry (with respect to a mirror plane along the high symmetry lines) in Fig. 2. White regions correspond to band gaps, gray regions to bulk bands and the δ-function-like dark streaks refer to localized surface states or high intensity surface resonances. While the overall agreement is very good there is a striking difference between the ASA and FP calculations at the $\bar{\Gamma}$ point, close to the Fermi level. Restricting the potential to a spherical shape leads to an attraction of the states which are around the $\bar{\Gamma}$ point, so that they fall below the Fermi level and become occupied. Here we should note that states with small $\mathbf{q}_\parallel$ vectors extend further away in the vacuum region since the decay length is proportional to $\exp[-(\kappa^2+q_\parallel^2)z]$, where κ is the decay length for normal incidence which is determined by the work function. This means that the ASA potential is too attractive for states which are located around the center of the two-dimensional (2D) Brillouin zone, and are the relevant ones for STM. This is a consequence of the spherical averaging of the surface potential barrier in the vacuum region, and such an approximation is more severe for states with a larger extent in the vacuum. Here we must note that the ASA error is rather small, but crucial for a discussion of tunneling spectra which probe states that extend far into the vacuum region. From now on we concentrate on full-potential results.

In order to simulate the STM spectrum by *ab initio* calculations, only states with $\mathbf{q}_\parallel < 1/6\bar{\Gamma}\bar{X}$ in the vicinity of the $\bar{\Gamma}$ point were considered in Ref. 8; thus only states with the slowest decay in the vacuum were probed. In this way a single peak in the LDOS in the vacuum region above the E_F was obtained, in agreement with the measured spectra. However by performing the integration over the whole 2D Brillouin zone, we observe two peaks, one just above E_F and a smaller one in the occupied states. These two peaks are present in both the FP-KKR (Fig. 1) and the FLAPW calculations (Fig. 3). The two *ab initio* calculations are in very good agreement with each other despite the fact that in the FLAPW calculation, especially in the spin-up channel, s-like size oscillations arising from the finite thickness of the slab (31 ML) can be seen. The decay of the two resonance states into the vacuum region is different, as can be seen in the FLAPW results in Fig. 3, where we show the LDOS at vary-

ing distances from the surface. The decay of the occupied peak is faster, and at 13.7 Å above the surface the intensity of the peak above E_F dominates the spectrum. However, the second smaller peak is a true feature of the calculated surface which is predicted by both *ab initio* methods, and probably a more detailed experimental investigation is required in order to resolve this point. The origin of the two peaks can also be identified from Fig. 2. Asymptotically, at large distances, only the very small $\mathbf{q}_\parallel$ values at the $\bar{\Gamma}$ point contribute to the spectrum yielding the STS peak above E_F, while the smaller peak just below E_F arises from states with larger $\mathbf{q}_\parallel$ vectors which decay faster in the vacuum region.

Being aware of the failure of the spherical potential approximation to describe the STM, we can also explain the misleading results of a recent calculation of Fang *et al.*[12] These authors calculated the LDOS using a spherical potential approximation on an Fe tip above an Fe(001) surface, and obtained a peak at 0.1 eV below the Fermi level. They explained their disagreement with the measured STS by a possible sample-tip interaction which was found to be strong enough for small distances. However this conclusion is in contradiction with the STM measurement where the spectra remained unchanged for a wide range of tip-sample separations.[7] From the above arguments it is clear that the measured STM spectrum for Fe(001) is not due to a possible tip-sample interaction, but represents an intrinsic feature of the Fe(001) surface.

IV. IMPURITIES IN Fe(001)

The magnetic properties and the energetics of $3d$ impurities in Fe(001) were studied previously.[10,17] Those calculations showed that Co and Ni ''prefer'' ferromagnetic alignment with respect to the substrate, while V and Cr align antiferromagnetically. The case of Mn is critical, since a Mn adatom couples ferromagnetically to Fe moments, while in the first surface layer the antiferromagnetic configuration has a lower energy. Additionally, with the exception of Co, for all $3d$ impurities the adatom configuration is unfavorable, and the impurities prefer to integrate into the first layer, presumably by the direct exchange mechanism.[10] Guided by the results of previous calculations, we perform only KKR calculations for impurities in the first surface layer. Lattice relaxation effects are ignored, since the relaxation of the outer surface layer of Fe(001) is small,[22,23] while previous calculations of our group[24] for impurities in bulk Fe showed that the size differences between $3d$ impurities and the Fe host atoms only lead to very small lattice distortions. In the present work, using a full-potential treatment we find that V, Cr, and Mn align antiferromagnetically to the Fe surface with moments of $-2.13\mu_B$, $-2.75\mu_B$, and $-3.38\mu_B$, respectively. Co and Ni atoms couple ferromagnetically with magnetic moments of $1.69\mu_B$ and $0.62\mu_B$, while the Fe surface atoms have moments of $2.78\mu_B$. These results for the magnetic moments are, as expected, in close agreement with previously published ASA results,[17] since the magnetic properties are rather insensitive to the form approximation of the potential.

The calculated LDOS at the impurity sites, as well as the LDOS of the pure Fe(001) surface, denoted by ''Fe in Fe,'' are shown in Fig. 4. One clearly notices the preferential filling of the minority band in the case of V, Cr, and Mn, indicating the antiferromagnetic coupling to the Fe surface, and the preferred filling of the majority band for Co and Ni impurities with ferromagnetic aligned moments. The majority band is either completely filled (for Co and Ni) or more or less empty (for V, Cr, and Mn) so that in all cases the LDOS around E_F is flat. In contrast to this, in the minority LDOS around E_F we observe similar peaks as the surface state peak for pure Fe. This analogy is particularly clear for V, Cr, and Co impurities. However, the peak position is shifted away from the surface resonance. The physical origin of these peaks will be discussed below.

STM can typically probe the electronic structure 1–2 eV around E_F, and for high-resolution imaging the tip scans the surface at a distance of 5–10 Å. Therefore the relevant states are only the ones with a large extent into the vacuum region, close to the Fermi level. In Fig. 5 we present the total LDOS for both spin directions close to the Fermi level on the Cr impurity site as well as on atomic sites centered at 2.75 and 5.5 Å above the defect. The distances are measured from the nucleus, and correspond to two and four times the interlayer distance respectively. Looking at the LDOS on the Cr site, we can see two resonances corresponding to the majority unoccupied state and the minority occupied one. Going 2.75 Å above the impurity the structure remains almost the same, with a smaller peak appearing just at the Fermi level. Moving further away from the surface at 5.5 Å, the unoccupied Cr d state is clearly seen at about $+1.3$ eV and a double-peak structure originating from the minority band shows up near E_F.

The position of the two (minority) peaks close to the Fermi level is in very good agreement with the STS experiment of Davies *et al.*,[8] who observed a double-peak structure on the tunneling spectrum when the STM tip was above the defect. They identified the defects as single Cr impurities in the surface layer, which is confirmed by our calculation. Comparing the positions of resonances at 5.5 Å , we conclude that the lower-energy peak is due to the impurity while the peak just above the Fermi level arises from the pure Fe surface, i.e., the Fe atoms close to the impurity. The relative increase of the Fe peak with respect to the Cr peak for larger distances is due to the fact that the tip probes the tunneling current over a large area, so that the relative weight of the Cr current decreases.

We can extract more information about the Cr impurity spectra from a symmetry decomposition of the calculated LDOS. In Fig. 6 we present symmetry decomposed density of states for Cr. The point-symmetry group of an impurity on the surface is C_{4v}. The impurity d state is split into irreducible representations of C_{4v}. We observe a Δ_1 component which locally projects to s, p_z, and d_{z^2} orbitals, a Δ_2 component, with a $d_{x^2-y^2}$ contribution, a Δ_5 component with a d_{xz} and d_{yz} admixture, and a $\Delta_{2'}$ state projecting into d_{xy}. At 2.75 Å above the impurity we see that the spectrum is dominated by the d_{z^2} states. The large resonance of the d_{xz} and d_{yz} characters has almost vanished in the second vacuum layer, while the $d_{x^2-y^2}$ character has already totally disappeared. Going 5.5 Å above the impurity we observe that only Δ_1 states contribute to the resonances. Thus these s-d_{z^2} states are responsible for the double-peaked structure seen in the STM measurements. Essentially STS probes states close

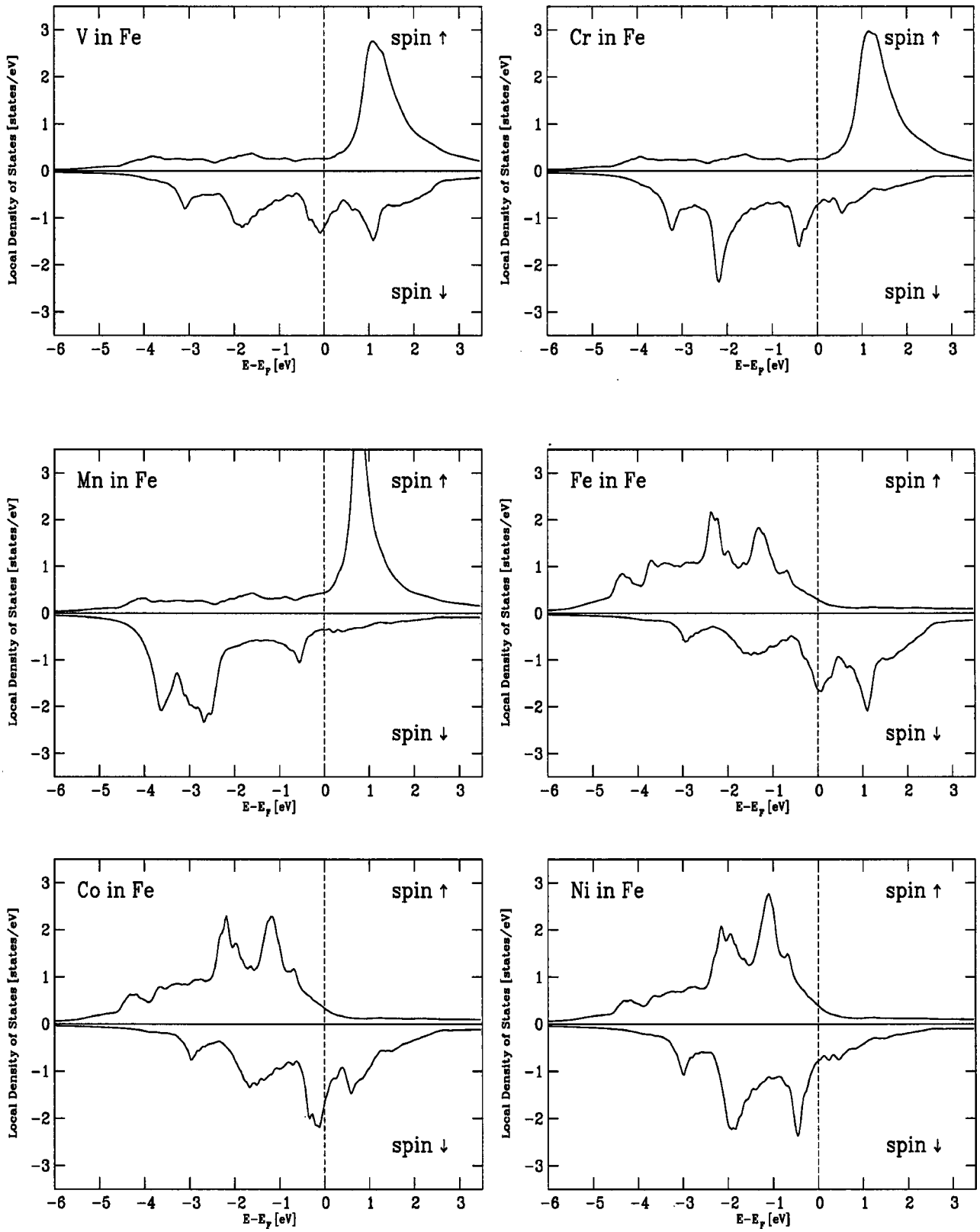

FIG. 4. Local density of states on the impurity site for majority- and minority-spin directions of 3*d* impurities V, Cr, and Mn and Fe, Co, and Ni embedded in the first layer of an Fe(001) surface calculated with the KKR method.

to the $\bar{\Gamma}$ point of the Brillouin zone, since these states have the slowest decay in the vacuum. As we see in Fig. 6, a small contribution from Δ_5 (d_{xz}-d_{yz}) orbitals is still seen even 5.5 Å away from the surface. However, this contribution is nonresonant, and forms an energy-independent background intensity. But these later states are responsible for the anticorrugation in the Fe(001) surface, as discussed in Ref. 20.

The different range of the impurity d_{z^2}, d_{xz}, and $d_{x^2-y^2}$ orbitals in the vacuum region can be understood as follows.

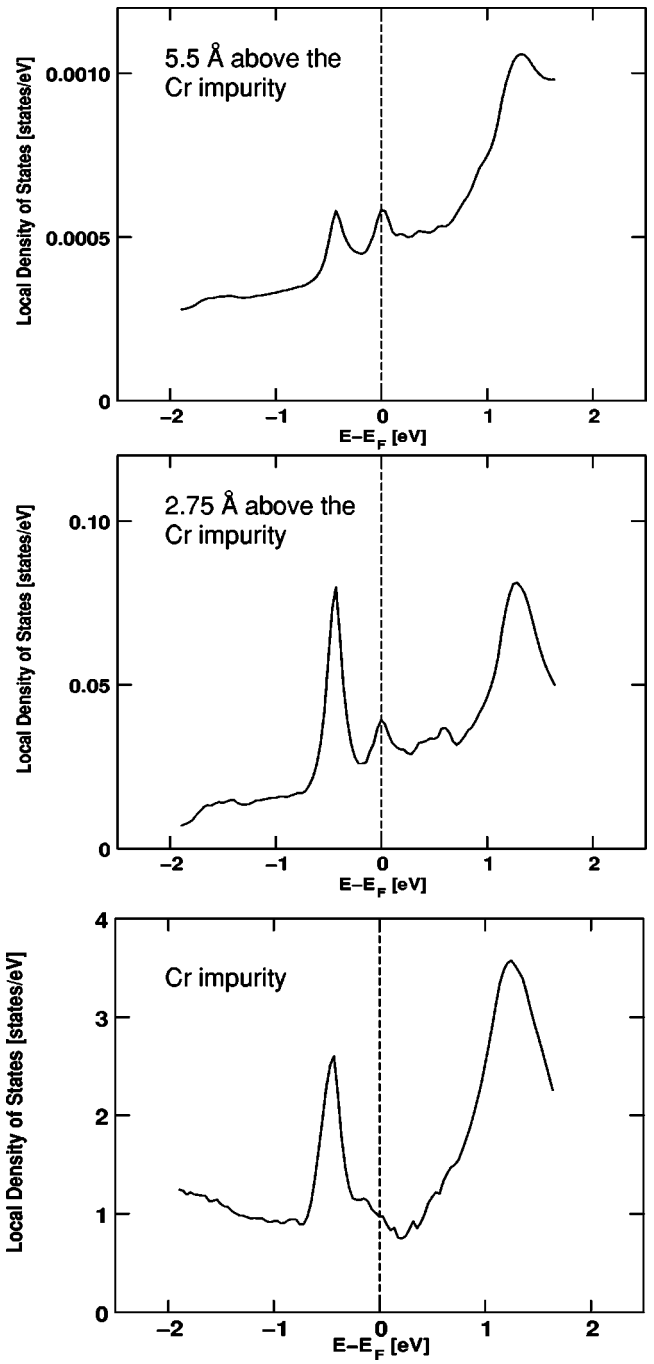

FIG. 5. Local density of states for both spin directions for Cr in Fe(001). From bottom to top, at the Cr site, 2.75 Å (second vacuum layer) and 5.5 Å above the impurity, and KKR calculation.

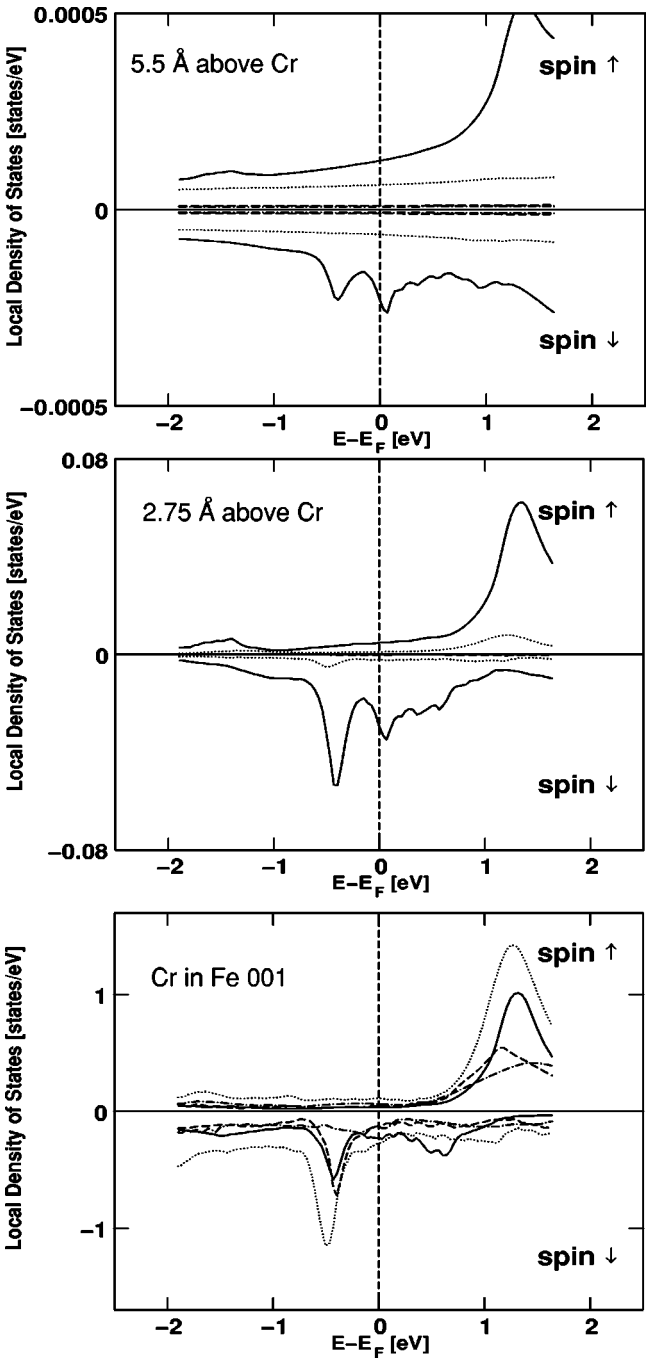

FIG. 6. Symmetry decomposition of the surface states for Cr in Fe(001). Impurity site and second vacuum layer (2.75 Å) and fourth vacuum layer (5.5 Å) above the impurity, calculated with the KKR method. Full line: Δ_1 symmetry, dotted line: Δ_5 symmetry, dashed line: Δ_2 dashed-dotted line, Δ_2 symmetry.

A d_{z^2} orbital pointing into the vacuum can be considered as a monopolar perturbation of the pure surface, spreading electrons into the vacuum region. In contrast to this, d_{xz} and d_{yz} orbitals act as in-plane dipole perturbations, while the $d_{x^2-y^2}$ orbital represents an in-plane quadrupole. Due to cancellation effects a dipolar (quadrupolar) perturbation decreases faster (much faster) in the vacuum than a monopolar contribution, which explains the behavior observed in Fig. 6.

If an impurity atomic level falls in the surface band region it will hybridize with the surface electrons. In the case of Fe(001) the *d* impurity states fall into the gap of the minority bulk band structure that causes the surface state above E_F. This means that the impurity d_{z^2} orbitals remain localized in the surface. These orbitals point toward the vacuum region and hybridize weakly with the Fe orbitals of the same symmetry, since the bcc(001) surface is not so closely packed and in-plane atoms are only second-nearest neighbors. However the corresponding orbital level d_{z^2} will in general be different from the surface level and will, due to the small half-width of the surface resonance, fall outside the surface band. Therefore, the corresponding state is three-

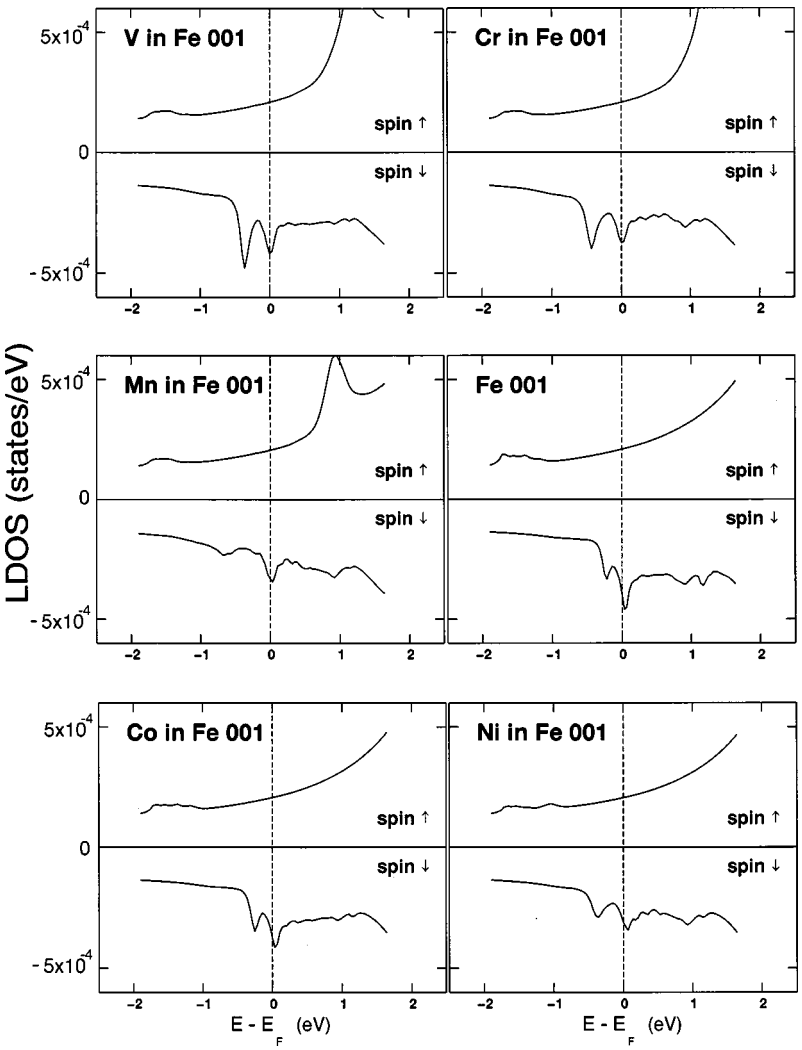

FIG. 7. Spin-resolved local density of states at 5.5 Å above $3d$ impurities in an Fe(001) surface calculated with the KKR method.

dimensionally localized and basically consists of a d_{z^2} orbital pointing into the vacuum region. It is also interesting to notice that although the d_{z^2} orbitals contribute only about one fifth of the total density of states (DOS) peak at the Cr site, they represent the only relevant contribution to the STS.

We have performed similar calculations for all $3d$ impurities, and the results for the spin-resolved LDOS at the vacuum site 5.5 Å above the impurities are presented in Fig. 7. The Fe(001) surface [''Fe(001)''] is shown here again for comparison. As one can see, not only Cr, but also V, Co, and Ni impurities show a similar double-peak structure in the minority band, which means that they can also be identified by their STS. Interestingly the case of Mn is somewhat different since our calculations give only a small, broader peak at lower energies. Comparing with Fig. 4, we see that for Mn the minority band has moved to lower energies, and that this peak is probably not accessible to STS. However, it might be possible to probe the strong peak in the majority-band state which is positioned about 1 eV above E_F.

We have also performed similar calculations for $4d$ impurities in the first layer.[18] In general, for these impurities the local moments and the resulting exchange splittings are much smaller. Therefore, for both bands many of these impurities exhibit LDOS peaks in the interesting energy region around E_F [for instance, the LDOS for a Ru impurity in the Fe(001) surface is shown in Fig. 2 of Ref. 18]. Therefore, we also expect similar peaks in the corresponding tunneling spectra. Thus we conclude that the occurrence of these peaks is a more general feature, and should in principle allow a chemical identification of most transition-metal impurities in the Fe(001) surface.

V. CONCLUSION

We have presented *ab initio* simulations of the STS for the Fe(001) surface and several $3d$ impurities in this surface. Our results can explain the measured spectra for both the clean surface[7] and Cr impurities on this surface.[8] We have demonstrated that a full-potential treatment is essential for an accurate description of the vacuum wave functions, while a spherical potential approximation might lead to incorrect results. Our calculations predict that the double-peak structure close to E_F, which is observed in the experiments for Cr, is present for many $3d$ impurities and can be used to identify foreign atoms in the (001)Fe surface. A symmetry decomposition of the LDOS shows that the STS peaks arise from d_{z^2} orbitals. We expect that similar features should also occur for $4d$ and $5d$ impurities.

ACKNOWLEDGMENTS

The authors would like to thank L. Szunyogh for confirming our ASA calculations for the Fe(001) surface by his KKR computer codes. This work was partially funded by the TMR Network ''Interface Magnetism'' of the European Union. Moreover we acknowledge support by the Schwerpunktprogramm ''Relativistic Effects'' of the Deutsche Forschungsgemeinschaft. Furthermore, one of us (S.H.) acknowledges support by the DFG under Grant Nos. BL444/1-1 and WI1277/6-1.

[1] F. Besenbacher, Rep. Prog. Phys. **59**, 1737 (1996).
[2] J. Tersoff and D. R. Hamann, Phys. Rev. B **31**, 805 (1985).
[3] M. Schmid, H. Stadler, and P. Varga, Phys. Rev. Lett. **70**, 1441 (1993).
[4] B. Voigtländer, V. Scheuch, H. P. Bonzel, S. Heinze, and S. Blügel, Phys. Rev. B **55**, R13 444 (1997).
[5] S. Heinze, S. Blügel, R. Pascal, M. Bode, and R. Wiesendanger, Phys. Rev. B **58**, 16 432 (1998).
[6] T. Jung, Y. W. Mo, and F. J. Himpsel, Phys. Rev. Lett. **74**, 1641 (1995).
[7] J. A. Stroscio, D. T. Pierce, A. Davies, R. J. Celotta, and M. Weinert, Phys. Rev. Lett. **75**, 2960 (1995).
[8] A. Davies, J. A. Stroscio, D. T. Pierce, and R. J. Celotta, Phys. Rev. Lett. **76**, 4175 (1996).
[9] A. Biedermann, O. Genser, W. Hebenstreit, M. Schmid, J. Redinger, R. Podloucky, and P. Varga, Phys. Rev. Lett. **76**, 4179 (1996).
[10] B. Nonas, K. Wildberger, R. Zeller, and P. H. Dederichs, Phys. Rev. Lett. **80**, 4574 (1998).
[11] S. Heinze, R. Abt, S. Blügel, G. Gilarowski, and H. Niehus, Phys. Rev. Lett. **83**, 4808 (1999).
[12] C. M. Fang, R. A. de Groot, M. M. J. Bischoff, and H. van Kempen, Surf. Sci. **436**, L648 (1999).
[13] R. Zeller, P. Lang, B. Drittler, and P. H. Dederichs, Mater. Res. Soc. Symp. Proc. **253**, 357 (1992).
[14] P. Lang, V. S. Stepanyuk, K. Wildberger, R. Zeller, and P. H. Dederichs, Solid State Commun. **92**, 755 (1994).
[15] S. H. Vosko, L. Wilk, and M. Nusair, J. Chem. Phys. **58**, 1200 (1980).
[16] N. Stefanou, H. Akai, and R. Zeller, Comput. Phys. Commun. **60**, 231 (1990); N. Stefanou and R. Zeller, J. Phys.: Condens. Matter **3**, 7599 (1991).
[17] B. Nonas, K. Wildberger, R. Zeller, and P. H. Dederichs, J. Magn. Magn. Mater. **165**, 137 (1997).
[18] B. Nonas, K. Wildberger, R. Zeller, and P. H. Dederichs, and B. L. Gyorffy, Phys. Rev. B **57**, 84 (1998).
[19] E. Wimmer, H. Krakauer, M. Weinert, and A. J. Freeman, Phys. Rev. B **24**, 864 (1981); M. Weinert, E. Wimmer, and A. J. Freeman, *ibid.* **26**, 4571 (1982).
[20] T. Asada, G. Bihlmayer, S. Handschuh, S. Heinze, Ph. Kurz, and S. Blügel, J. Phys. C **11**, 9347 (1999); S. Heinze, X. Nie, S. Blügel, and M. Weinert, Chem. Phys. Lett. **315**, 167 (2000).
[21] We found that the exact shape of the LDOS in the vacuum region changes with the l_{max} cutoff. Fortuitously, the ASA $l_{max}=2$ results for the first vacuum layer LDOS are very similar to the FP $l_{max}=3$ calculations. However, the ASA always gives the peak position below the Fermi level, as can be observed going further away from the surface. Our result was also confirmed by Dr. L. Szunyogh by using his KKR surface codes. This feature of ASA also persists for the experimental lattice constant.
[22] S. Handschuh and S. Blügel, Solid State Commun. **105**, 633 (1998).
[23] F. Jona, Surf. Sci. **68**, 204 (1977).
[24] T. Korhonen, N. Papanikolaou, R. Zeller, and P. H. Dederichs, Philos. Mag. B **78**, 429 (1998).